PANAMGEO CHILE 2024
17th PAN-AMERICAN CONFERENCE ON SOIL MECHANICS AND GEOTECHNICAL ENGINEERING | 2nd LATIN-AMERICAN REGIONAL CONFERENCE OF IAEG
LA SERENA • CHILE / NOVEMBER 12 - 16, 2024

Proceedings of the 17th Pan-American Conference on Soil Mechanics and Geotechnical Engineering (XVII PCSMGE), and 2nd Latin-American Regional Conference of the International Association for Engineering Geology and the Environment (IAEG), La Serena Chile, 2024.

Recent research advances in the characterization of contractive tailings with the cone penetration test within the critical state soil mechanics framework

Avances recientes de investigación en la caracterización de relaves contractivos con el ensayo de penetración de cono dentro del marco de la mecánica de suelos de estado crítico

Juan Ayala
Tailings Engineering, KCB Australia Pty Ltd, Australia, jlayalat@gmail.com

Andy Fourie
School of Engineering, The University of Western Australia, Australia

ABSTRACT: Recent tailings storage facility (TSF) failures have driven renewed interest in the appropriate characterization and assessment of these facilities over the last few years. The cone penetration test (CPT) is one of the most commonly used tools by practitioners to infer tailings properties within these facilities; however, different correlations are needed in order to infer these properties from the mechanical resistances recorded by the CPT probe advance within the ground. Most of these CPT correlations widely available in the literature are based on laboratory-controlled calibration chamber (CC) testing, which is arguably the most trusted method to correlate the tailings of different states to the CPT-acquired data. Unfortunately, these CC databases are mainly composed of clean sands usually prepared at much denser states (i.e. dilative) than those found in conventional TSFs (i.e. contractive) that also tend to store finer gradations when compared to the sands from historical CCs databases. This work presents CC data tested at the University of Western Australia in an in-house developed small-scale CC, where silty tailings were prepared at contractive states and tested in drained conditions, presenting an updated assessment when compared to other tools commonly used in practice. Additionally, a novel methodology to infer the state parameter for partially drained penetration conditions is presented.

KEYWORDS: CPT, Calibration chamber, State parameter, Partial drainage, Soil behavior-type index.

1 INTRODUCTION.

The characterization of tailings storage facilities (TSF) has become an important subject during the last few years, as new global standards (ANCOLD, 2019; ICMM, 2020) have emerged driven by the latest catastrophic failures (ICOLD, 2001; Fourie et al., 2001; LePoudre, 2015; Morgenstern et al., 2015; Riveros and Sadrekarimi, 2017; Morgenstern, 2018; Robertson et al., 2019; CIMNE, 2021). When considering that in previous decades, TSFs were mostly treated as a negligible part of the mining process, it is understandable why not many as-built drawings or construction controls records can be found when assessing the stability of some of these old structures. Here is where the cone penetration test (CPT) can play a key role.

An additional subject that has reemerged lately, is which technology or framework practitioners use when assessing the stability of these usually loose structures. Here, the critical state soil mechanics (CSSM) approach (Wood, 1991; Verdugo and Ishihara, 1996; Fourie and Papageorgiou, 2001; Jefferies and Been, 2015) has been placed in the spotlight especially due to its capacity to explain some of the mechanical processes of loose granular materials, in particular, with the state parameter (ψ) concept introduced by Been and Jefferies (1985) almost four decades ago, is becoming a common tool between practitioners and researchers.

This work presents a summary of some of the findings on the CPT-ψ correlations for loose silty tailings developed at The University of Westen Australia, within the TAILLIQ research project (Fourie et al., 2021).

1.1 *The CPT and the ψ*

The CSSM approach has become the go-to technology to predict the soil behavior at shearing in most TSFs, especially upstream dams (Vick, 1990), and the ψ a key measurement that directs later soil assessments, including if the structure stability will be assessed with undrained peak and residual properties. In other words, the ψ will direct how much the engineer will stress the assessment of the soil structure. The ψ for dilative and contractive states, and the critical state line (CSL) are presented in Figure 1.

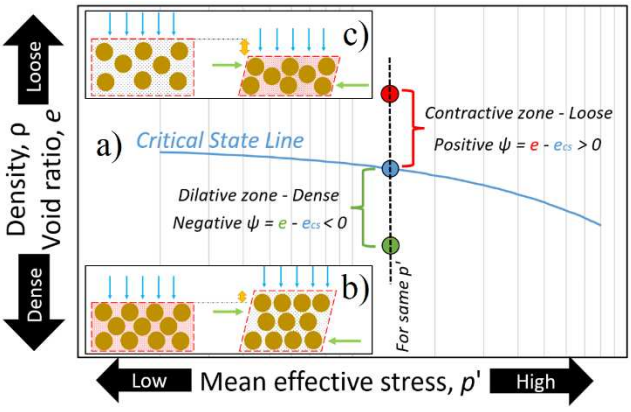

Figure 1 a) Critical state line including b) dilative, and c) contractive particles behavior during shearing.

The CSL shown in Figure 1a), corresponds to a combination of void ratio and mean effective stress where the soil will shear with a steady state, this is, where no additional driving forces are needed to continue shearing, and no further volume or pore water pressure changes are recorded. As noted in the figure, the CSL can be curved, generally at stresses over 1 MPa (Verdugo and Ishihara, 1996; Jefferies and Been, 2015), however, this is material dependent, so its characterization must target the stress range of each project. The CSL also separates two different volumetric behaviors at shearing, the dilative-volume expansion when below the CSL (Figure 1b), and the contractive-volume reduction when above the CSL (Figure 1c).

As shown in Figure 1a), a positive ψ means a contractive state, where the volume reduction (Figure 1c) can generate excess pore pressures if the voids are saturated, or re-saturate a partially saturated material. Conversely, a negative ψ means that dilation will govern soil shearing, nonetheless, since dilation is in itself a loosening process (Figure 1b), new ψ and stability reassessments may be needed after considerable loads, as further raises or large earthquakes, among other possible factors, as reflected in the simplified flow chart of soil liquefaction of the CANLEX project (Robertson et al., 2000) shown in Figure 2.

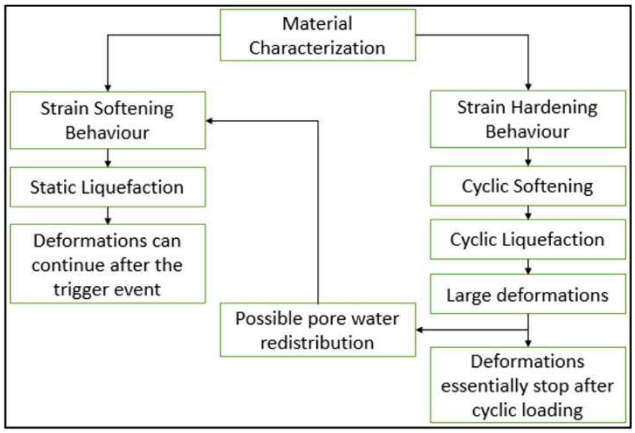

Figure 2 Simplified flow chart of soil liquefaction according to the CANLEX project (modified after Robertson et al., 2000).

When inferring the ψ with the CPT, usually one form of the normalized tip resistance (Q_p or $Q_p(1-B_q)+1$, for details see Jefferies and Been (2015)) will be used along with some calibrated method (Plewes et al., 1992; Shuttle and Jefferies, 1998; Shuttle and Cunning, 2007; Ghafghazi and Shuttle, 2008; Robertson, 2010; Shuttle and Jefferies, 2016). Material-specific correlations are recommended especially at contractive states, due to large ψ variability, as shown in Figure 3, where a $Q_p = 30$ can infer dilative or contractive states, depending on the characterization/correlation used, leading to different assessment methods as previously discussed.

2 MINI CALIBRATION CHAMBER.

To obtain these site-specific correlations, calibration chambers (CC) are usually the recommended method, as the CPT can be pushed into the soil under laboratory-controlled conditions. CCs are in many ways enlarged triaxial devices, where different sample preparation methods can be used to reach different densities, consolidate to different stress conditions with varied degrees in saturation (Russell et al., 2024), to finally, instead of shearing the sample as in a conventional triaxial test, the CPT is pushed into the sample, allowing to correlate the CPT recorded data to the known soil state. By testing the same material at different initial ψs, correlation trends as those shown in Figure 3 can be obtained.

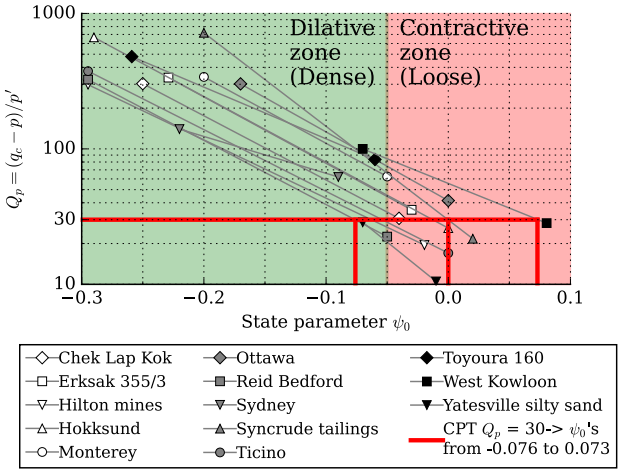

Figure 3 Different correlations for CPT-ψ depending on the selected material (data from Jefferies and Been, 2015).

The University of Western Australia, within the TAILLIQ research project developed two CPT-CCs, a small CC by modifying a triaxial device (Ayala et al., 2020a, 2021), also known as the MiniCal, and a large CC (Ayala et al., 2020b), also known as the BigCal. The findings made with the MiniCal device, shown in Figure 4, are discussed on this section.

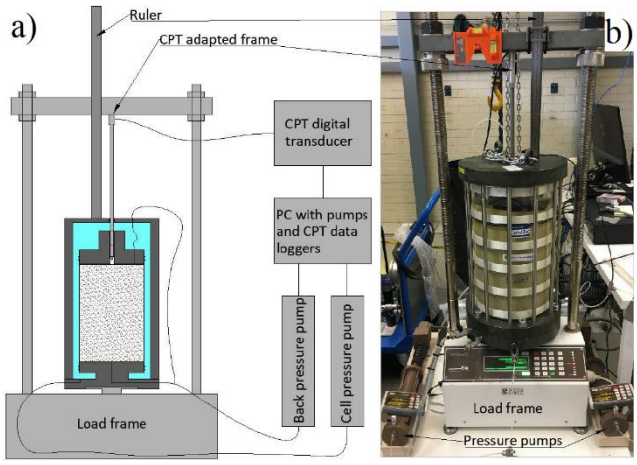

Figure 4 a) MiniCal general scheme, and b) photo during testing.

The MiniCal can allocate samples of 20 cm in diameter and 30 cm height, and test using two different cones with 6 mm and 10 mm in diameter. The smaller sample size, in comparison to larger CCs (Houlsby and Hitchman, 1988; Huang, 1991; Holden, 1991;

Ghionna and Jamiolkowski, 1991; Been et al., 1986, 1987; P. K. Robertson and Campanella, 1983; P. Robertson and Campanella, 1983) allows for careful preparation of samples at very loose states, as with the undercompaction method (Ladd, 1978), making easier to test samples in contractive states. Some MiniCal normalized test records are presented in Figure 5.

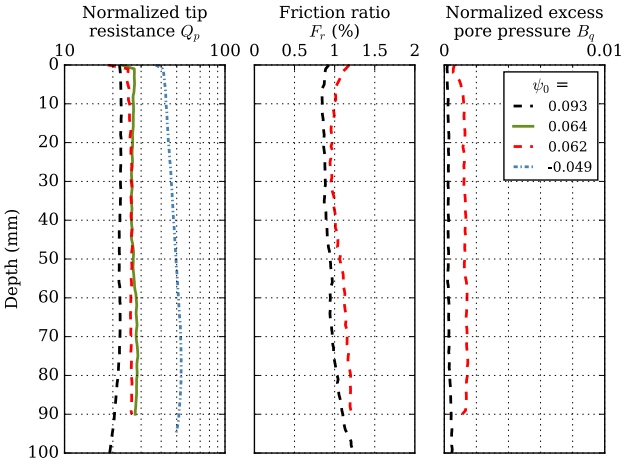

Figure 5 MiniCal normalized penetration records for some test on Gold tailings at different initial ψs (Ayala et al., 2020a).

2.1 *MiniCal results comparison to simulation methods*

Ayala et al. (2020a) presented results for two silty tailings, of an Australian Gold tailings, and a South African Platinum tailings. The MiniCal correlation results can be seeing in Figure 6 for these two materials.

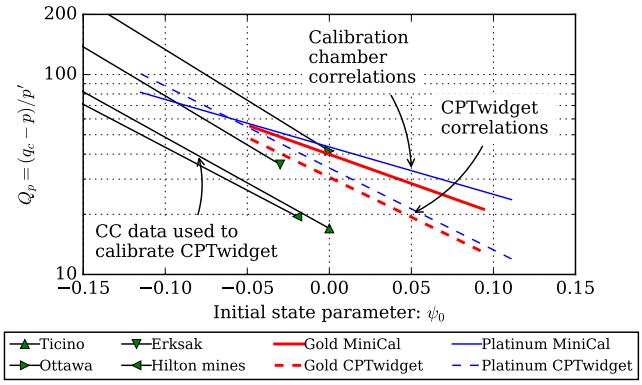

Figure 6 Different CPT-ψ correlations for the MiniCal results, the CPTwidget simulation results, and the materials used to calibrate the CPTwidget scaling.

Figure 6 also presents with dashed lines the CPTwidget (Shuttle, 2019) simulation results for both tailings. The CPTwidget uses the NorSand constitutive model (Jefferies and Shuttle, 2005) with the spherical cavity expansion method, to calculate CPT correlations. However, since a sphere expanding has a different soil response than a CPT probing the soil, as shown for Ticino sand data in Figure 7a), a scaling rule is needed to make the spherical simulation results work for CPT correlations (Figure 7b).

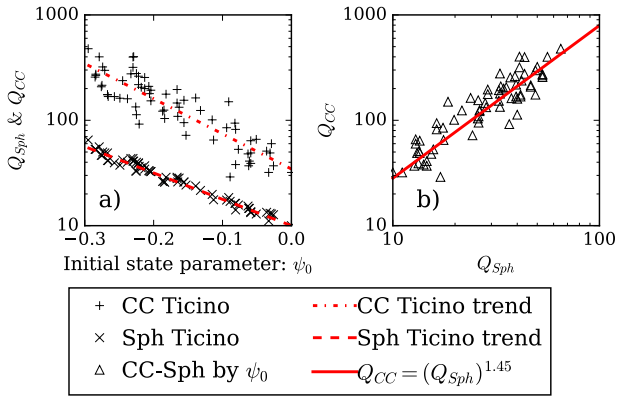

Figure 7 a) CC and Spherical cavity expansion simulations for the database of Ticino sands, and b) a scaling equation previously used to correct for geometry.

Nonetheless, since the scaling rule currently used in the CPTwidget is calibrated to a mainly dilative database of the four materials shown with triangle markers in Figure 6, the scaled CPTwidget results tend to have a similar slope/response to those materials, having to extrapolate the scaling/correction into the contractive behavior region, generating unconservative correlations for both materials. Aiming to correct for this unconservative extrapolation in the contractive region, the rescaling equation shown in Figure 8 was inferred by calculating the ratio between the MiniCal results (Q_{CC}) over the CPTwidget results ($Q_{CPTwidget}$), and fitting an exponential equation when plotting these ratios against their initial ψ, based on the updated procedure presented by Shuttle and Jefferies (2016).

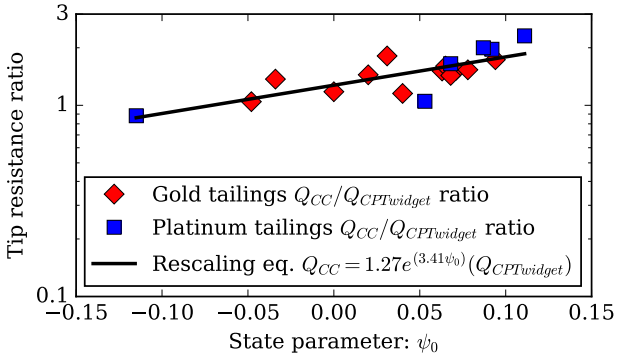

Figure 8 Rescaling equation fitting by plotting the $Q_{CC}/Q_{CPTwidget}$ ratio versus the initial ψ of each Gold and Platinum MiniCal test.

To assess the applicability of the rescaling equation, Ayala et al. (2023a) rescaled an updated correlation for the Canadian Lead and Zinc tailings originally presented by Shuttle and Cunning (2007), a comparison of these correlations is shown in Figure 9.

The relevance of this Canadian tailings, is that in addition to the CPT data, includes ψs independently calculated from recovered saturated samples. Also, that when combining the data in the Shuttle and Cunning (2007) and Shuttle and Jefferies (2016)

works, an updated set of NorSand parameters is available for CPTwidget simulations. Figure 9 shows with the black dotted line the correlation for the original 2007 publication, in the blue dashed line the correlation simulated with the 2016 publication and updated CPTwidget version, and in the red solid line the 2016 correlation rescaled using the equation presented in Figure 8 for ψ ≥ -0.05, with the hatched area as the main target for the rescaling method.

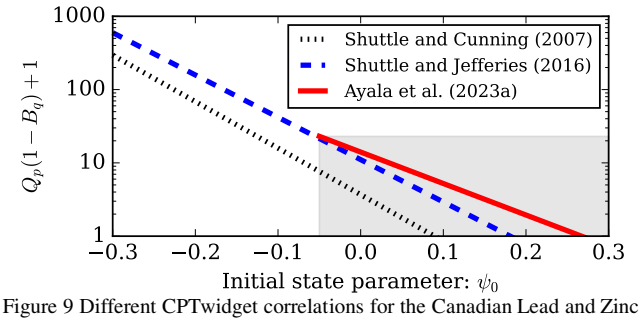

Figure 9 Different CPTwidget correlations for the Canadian Lead and Zinc tailings, including the rescaled for ψ ≥ -0.05.

It is noted that while the NorSand constitutive model and the CPTwidget scaling rule have being updated since the Shuttle and Cunning (2007) publication (Shuttle, 2019; Shuttle and Jefferies, 2023; Ayala et al., 2023b), Ayala et al. (2023a) showed an improved match between the ψs calculated from the recovered samples (black squares in Figure 10c) and the ψs inferred from the CPT data (same line styles as Figure 9) with the rescaled correlation.

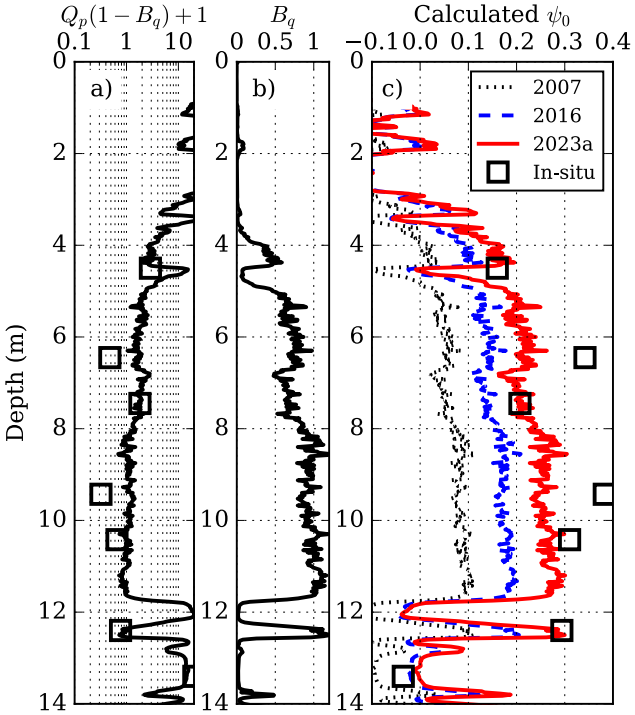

Figure 10 Different ψs in depth, inferred using Figure 9 correlations.

The black squares in Figure 10a) represent the required $Q_p(1-B_q)+1$ values to infer the ψ from the samples in Figure 10c), showing that for the non-matched samples at ~6.5 and ~9.5 m, a drop in the $Q_p(1-B_q)+1$ was needed to infer those values.

Alternatively to the spherical cavity expansion method, and taking advantage of recent years developed numerical methods, Ayala et al. (2023d) simulated axisymmetric models of the MiniCal with the open source software Anura3D (2022), with an implementation of the NorSand constitutive model (Martinelli and Galavi, 2022) for the Gold and Platinum tailings. Anura3D takes advantage of the material point method (MPM) to properly model large deformations in soil mechanics. The suitability of MPM for large-deformation analysis of CPT testing in soils has been shown by several recent studies (Ghasemi et al., 2018; Martinelli and Galavi, 2020; Martinelli and Pisanò, 2022). It uses the 'moving mesh' concept to ensure fine discretization around the soil-cone interface, with four-node quadrilateral elements. The mesh and some simulation outputs are shown in Figure 11.

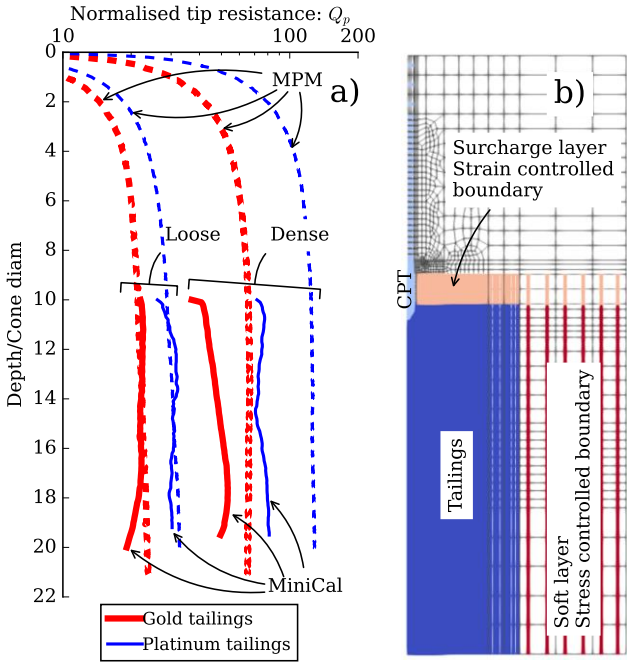

Figure 11 a) MiniCal and MPM results mirroring some Gold and Platinum initial states, and b) Axisymmetric MPM model mesh.

As can be seeing in Figure 11a), the loose-most contractive MPM simulations, mirrored the behavior from the MiniCal tests with the same initial ψ on both tailings, while for the initially denser states the simulations overpredicted the soil response. All MiniCal, CPTwidget, and MPM simulations are shown in Figure 12, where the MPM suitability especially for higher ψ is clear.

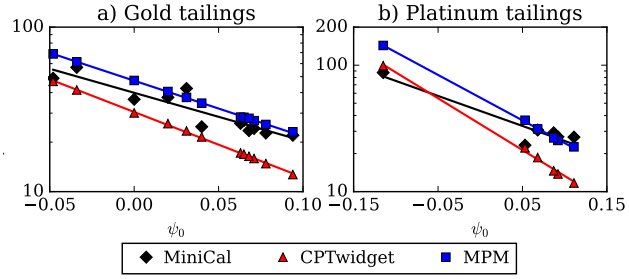

Figure 12 MiniCal, CPTwidget, and MPM simulation results comparison for the Gold and Platinum tailings.

3 PARTIAL DRAINAGE IN CPT TESTING.

When inferring geotechnical properties from CPT data in saturated materials, is noted that most correlations are developed for drained sand-like, or undrained clay-like materials. The problem is that many TSFs store silt-like materials that can respond in a partially drained manner to standard CPT probing, leaving practitioners with the decision of using drained or undrained correlations to infer soil properties as the ψ shown in Figure 13.

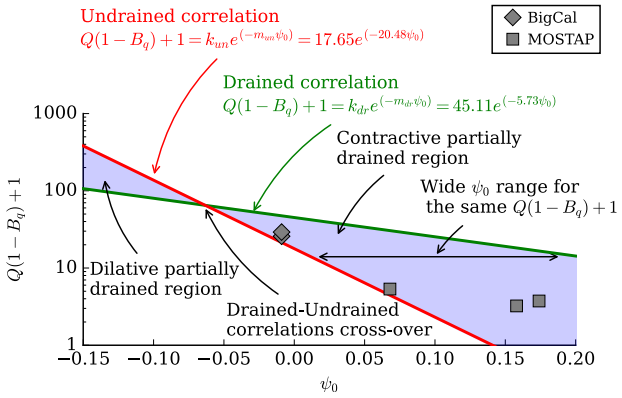

Figure 13 Drained and undrained CPT-ψ correlations for the Platinum tailings, showing the laboratory BigCal and in-situ MOSTAP samples in the contractive partially drained region.

As can be seeing in Figure 13 for the Platinum tailings, depending on the drainage assumption, the CPT will generally infer different ψs for the same material, with the exception been near the Drained-Undrained correlations cross-over. As shown in Figure 13 for a $Q(1\text{-}B_q)+1 \simeq 14$, the ψ interpretation can vary between ~0.01 to ~0.19, showing that the largest variations occur for the lowest CPT values, as tend to happen in most conventional TSFs.

In between the drained and undrained correlations in Figure 13, are two hatched regions with partially drained behavior. On the right side of the cross-over, is the contractive partially drained region, and on the left side, the dilative partially drained region. Now, understanding that for saturated materials, a drained or undrained response will depend on both, the soil properties (e.g. permeability, coefficient of consolidation), and perturbance characteristics (e.g. CPT penetration rate, CPT diameter), the characteristic curve concept (DeJong and Randolph, 2012) shown in Figure 14 comes in handy to assess the CPT response variation between drained, partially drained, and undrained scenarios.

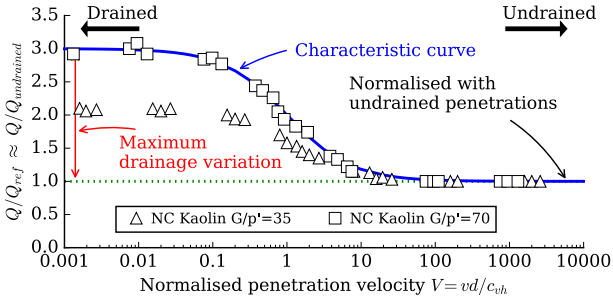

Figure 14 Characteristic curve approximation, and CPT data for two loose-normally consolidated Kaolin clays (for details see Yi et al., 2012).

Figure 14 presents CPT records for two sets of normally consolidated Kaolin clays with different rigidity indexes, over a large variety of Normalized penetration velocities (V). V is a dimensionless parameter that includes the CPT penetration rate (v), the cone diameter (d), and the coefficient of consolidation (c_{vh}) in the vertical or horizontal direction, whichever is faster, hence, controls the excess pore pressure dissipation.

Figure 14 also presents a characteristic curve adjusted for the data in square markers, however by changing the 'maximum drainage variation' shown on the drained-left side of the figure, the characteristic curve could also approximate the data in the triangle markers. Following this logic, Ayala et al. (2023c) compiled CPT data available in the literature from both, dilative (Silva and Bolton, 2005), and contractive data (Dienstmann et al., 2018; Finnie and Randolph, 1994; Yi et al., 2012), as shown in Figure 15 a) and b) respectively.

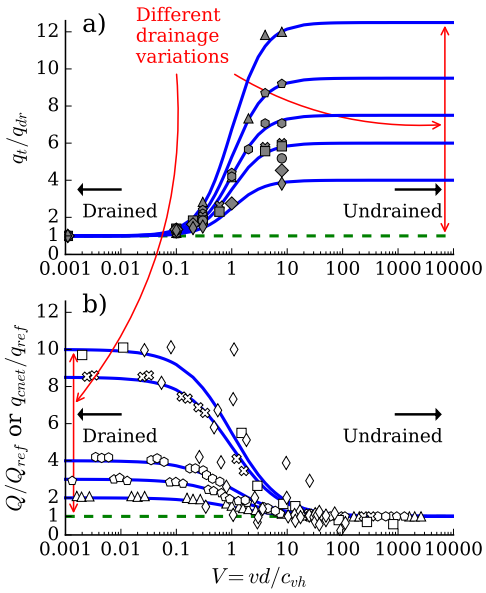

Figure 15 Literature compilation of CPT data over a range of different normalized penetration velocities, going from fully drained to fully undrained, separated in a) for dilative, and b) for contractive data.

In both Figure 15 graphs, a dashed line at unity represents the different drainage regimes selected to normalize each data, in Figure 15 a) the drained regime was originally used to normalize the dilative data, and in Figure 15 b) the undrained regime was originally used to normalize the contractive data. Aiming to use one expression to approximate both contractive and dilative behaviors, including all different maximum drainage variations, two modifications were proposed by Ayala et al. (2023c) to standardize the data in Figure 15. First, the drained regime was selected as the standard normalization regime, independent of the ψ of the material, and second, a percentage representation was used for all data, independent of the maximum drainage variation, using 0% for the drained regime, and 100% for undrained. These standardized graphs are shown in Figure 16 a) for the dilative data, and in Figure 16 b) for the contractive data.

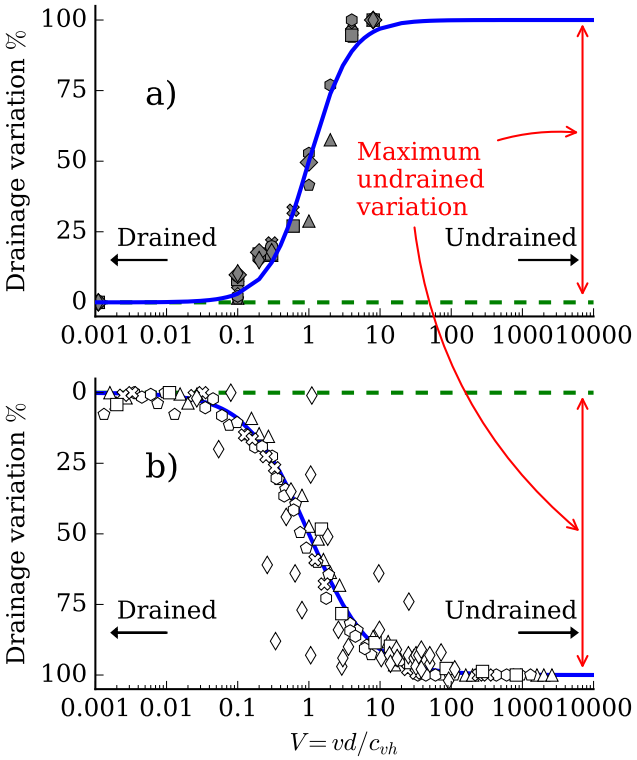

Figure 16 Percentage normalization of the data presented in Figure 15, using the drained regime as 0%, and undrained as 100 %, to fit a unique characteristic curve, with the dilative data presented in a) and the contractive in b).

The main thing to note in Figure 16 are the constant values of the characteristic curve on each side of both graphs, these fully drained/undrained plateaus allow for the combination of the standardized characteristic curves concept, with the CSSM CPT-ψ framework, by connecting these plateaus to their respective CPT-ψ drained/undrained correlations presented in Figure 13. The unification of these two frameworks permitted the creation of the characteristic surface concept presented in Figure 17.

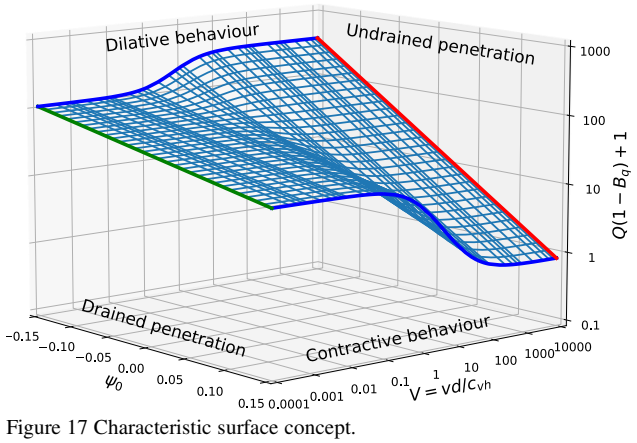

Figure 17 Characteristic surface concept.

The characteristic surface equation is presented in (1).

$$Q(1-B_q)+1 = \frac{\left(k_{un}e^{(-m_{un}\psi_0)} - k_{dr}e^{(-m_{dr}\psi_0)}\right)}{1+(V_{50}/V)^c} + k_{dr}e^{(-m_{dr}\psi_0)} \quad (1)$$

In equation 1, $Q(1\text{-}B_q)+1$, k_{un}, m_{un}, k_{dr}, m_{dr}, and ψ_0 were introduced in Figure 13, V introduced in Figure 14, and V_{50} and c are constants from the characteristic curve, both taken as unity by Ayala et al. (2023c), where a simplified methodology with the ψ-isolines shown in Figure 18 is suggested. Additionally, a detailed derivation of the characteristic surface concept is presented in Appendix H of Ayala (2022).

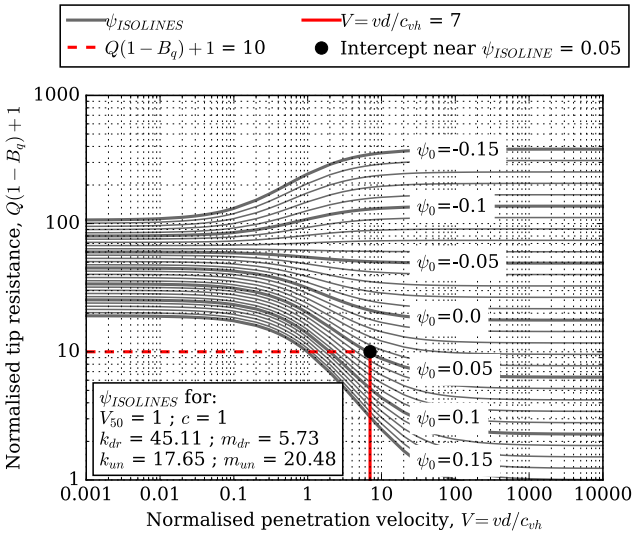

Figure 18 Inferring the ψ_0 with the characteristic surface ψ-isolines.

It must be noted that when using the characteristic surface and ψ-isolines methodology, it is required to know the coefficient of consolidation (c_{vh}) as shown in the Figure 18 example. Ayala et al. (2023c) used a method presented by DeJong and Randolph (2012) to infer the coefficient of consolidation from partially drained

dissipation tests. However, this method requires to assume how much partially drained the dissipation tests is, adding another variable into the problem. Ayala et al. showed that a 50% assumption gave an appropriate approximation when assessing the dissipation tests from the Platinum tailings recorded in the BigCal and In-situ, as shown in Figure 19.

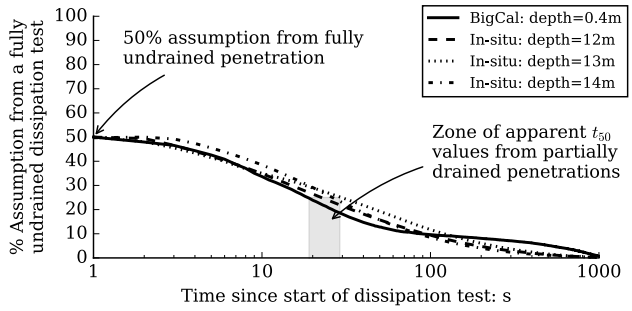

Figure 19 Dissipation tests of the BigCal and In-situ CPTs.

The relevance of the dissipation tests in Figure 19 is that the ψ in the BigCal was known at the time of probing, and during the In-situ testing, MOSTAP saturated samples were collected allowing to calculate the void ratio and ψ. The CPT-ψ relation for the BigCal and MOSTAP samples was presented in Figure 13, and the comparison for the in-situ testing between the ψs calculated from MOSTAP samples and the values inferred from the ψ-isolines are presented in Figure 20.

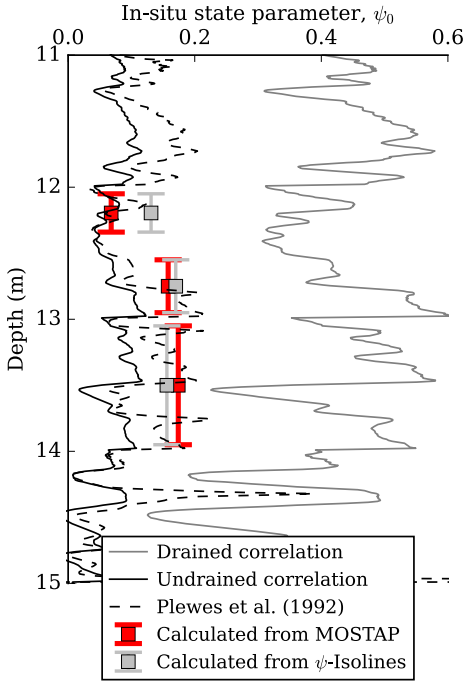

Figure 20 Platinum tailings ψs estimated from MOSTAP samples, the ψ-isolines and the partially drained dissipation test in Figure 19, the drained/undrained correlations in Figure 13, and Plewes et al. (1992).

Additionally, when Ayala et al. (2023c) showed that the percentage normalization of the literature data could be approximated with V_{50} = 1 and c = 1, also limited the c_{vh} range where partially drained dissipations could be expected to occur. Figure 21 presents the hatched region between c_{vh} ~80 to ~6500 mm²/s, where at least 10% of partially drained effects could be measured with the CPT.

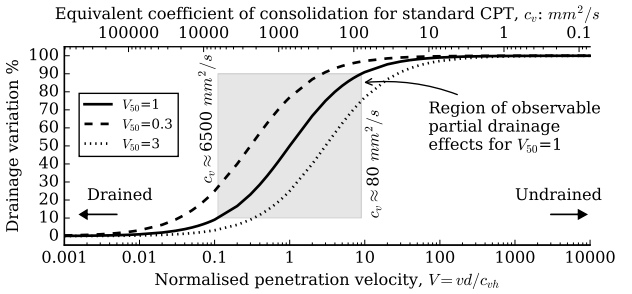

Figure 21 c_{vh} range where at least 10% of partially drainage effects are expected to be measured by the CPT.

Alternatively to the need of a c_{vh} value, Ayala et al. (2024) proposed a variation of the drainage regime by using the soil behavior-type index (I_c). For this, all CPT data with $I_c \leq 2.20$ is considered drained (i.e. $\%I_c = 0\%$), all CPT data with $I_c \geq 2.58$ is considered undrained (i.e. $\%I_c = 100\%$), and all in-between I_c values vary with a linear relation in percentage terms. This simplified method can be easily written in a spreadsheet, with the $\%I_c$ changing behavior with an If statement, and the later use of equation (2) to infer the ψ. All other parameters are already known from equation (1), and the I_c drained and undrained limits are presented over the soil behavior-type chart in Figure 22.

$$\psi = \frac{-\ln\left(Q(1-B_q)+1/k_{dr}\right)}{m_{dr}} + \%I_c \times \left(\frac{-\ln\left(Q(1-B_q)+1/k_{un}\right)}{m_{un}} + \frac{\ln\left(Q(1-B_q)+1/k_{dr}\right)}{m_{dr}}\right) \quad (2)$$

Figure 22 also presents two typical scenarios that tailings practitioners work with, first, silt-like paste thickened tailings that plot between the drained/undrained regions, and second, frequent interactions of sand-like and clay-like tailings. In the first case, the drained/undrained correlations for the silt-like material can be input in equation (2), and in the second case, the drained correlation of the sand-like material, with the undrained correlation of the clay-like material can be input in equation (2), giving the versatility to the practitioner to even modify the I_c limits if needed.

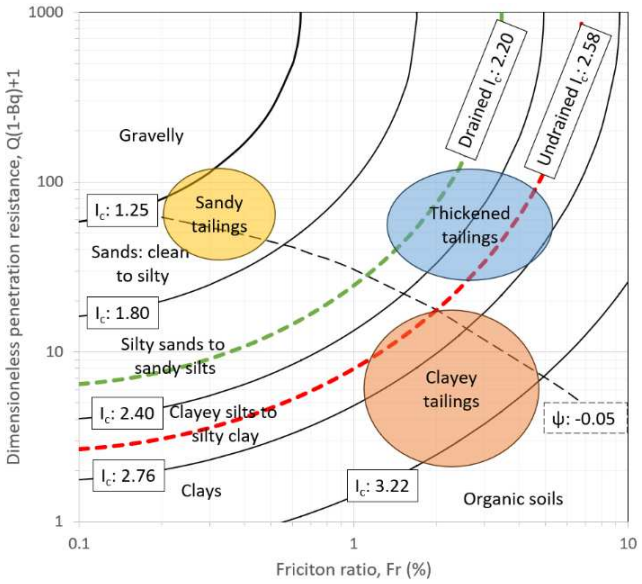

Figure 22 Soil behavior-type chart with the proposed I_c drained and undrained limits.

To review the behavior of equation (2), the synthetic CPT shown in Figure 23 was created, with a) an increasing $Q(1\text{-}B_q)+1$ in depth, and b) zig zag I_c values moving between fully drained and undrained. Here, a correct If statement implementation in excel will calculate an $\%I_c$ as the one shown in Figure 23 c), and will infer the ψ shown in d) with the solid line. Figure 23 d) also shows in dashed lines the fully drained and undrained ψ values for the CPT in a).

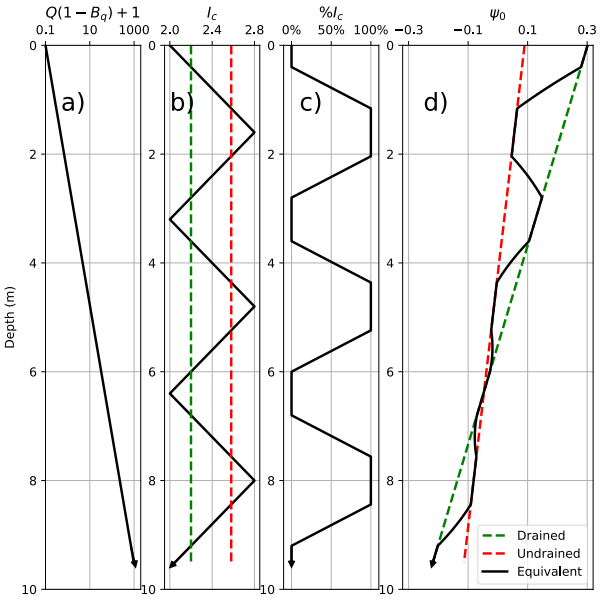

Figure 23 Synthetic CPT with (a) constantly increasing $Q(1\text{-}B_q)+1$ with depth, (b) variable I_c between drained and undrained limits, (c) percentage representation of the drained and undrained responses based on the I_c, and (d) the inferred ψ.

4 CONCLUSIONS

From all the works summarized in this paper, the general conclusions are as follows:

- Calibration chambers are the preferred method to infer CPT correlations, and smaller devices should be preferred when the soil conditions and the magnitude of the projects allows for this level of detail.
- Most CPT correlations are calibrated against data tested at denser states than those usually found on most tailings storage facilities, having to extrapolate these relations into the contractive region. These extrapolations were found unconservative, as they infer denser state parameters than those measured in laboratory-controlled calibration chambers.
- Newer numerical methods with large deformation capabilities, such as the material point method, permit to proper simulate the CPT behavior in the most contractive tests of the calibration chamber, showing promising capabilities for highly contractive facilities. While the method overpredicted the response at the denser test, this is considered conservative, and is still a preferred method in comparison to the extrapolation of current correlations into the contractive region.
- Two novel methods to infer the state parameter in partially drained conditions were introduced, the characteristic surface with the state parameter-isolines, and a simplified method based in the soil behavior-type index. Both methods were shown useful tools for practitioners.

5 ACKNOWLEDGEMENTS

The authors acknowledge the important contributions of Dr David Reid in the development of this research, including the development of the small calibration chamber.

The authors acknowledge the important support from ConeTec and Klohn Crippen Berger in the sponsorship of the small calibration chamber. This work was part of TAILLIQ (Tailings Liquefaction), which is an Australian Research Council (ARC) Linkage Project supported by financial and in-kind contributions from Anglo American, BHP, Freeport-McMoRan, Newmont, Rio Tinto, and Teck. The TAILLIQ project was carried out at The University of New South Wales, The University of South Australia, The University of Western Australia (lead university), and The University of Wollongong. We acknowledge the support and contributions of project personnel at each of the supporting organizations.

6 REFERENCES

ANCOLD, 2019. Guidelines on Tailings Dams - Planning, Design, Construction, Operation and Closure.

Anura3D MPM Research Community, 2022. Anura3D Version 2022 Source Code.

Ayala, J., 2022. Assessment of the state parameter in mine tailings using cone penetration tests with calibration chambers, Doctoral Thesis. The University of Western Australia.

Ayala, J., Fourie, A., Reid, D., 2023a. Example Application of the Rescaling Equation for CPT Inferred State Parameters in

Loose Mine Tailings. Int. J. Geomech. 23, 06023008. https://doi.org/10.1061/IJGNAI.GMENG-8040

Ayala, J., Fourie, A., Reid, D., 2023b. Reply to the discussion by Shuttle and Jefferies on "Improved cone penetration test predictions of the state parameter of loose mine tailings." Can. Geotech. J. https://doi.org/10.1139/cgj-2023-0095

Ayala, J., Fourie, A., Reid, D., 2023c. A Unified Approach for the Analysis of CPT Partial Drainage Effects within a Critical State Soil Mechanics Framework in Mine Tailings. J. Geotech. Geoenvironmental Eng. 149, 04023036. https://doi.org/10.1061/JGGEFK.GTENG-10915

Ayala, J., Fourie, A., Reid, D., 2021. Cone penetration testing of gold tailings in a small calibration chamber, in: Williams, D. (Ed.), . Presented at the Mine Waste and Tailings 2021 conference, The Australasian Institute of Mining and Metallurgy, Brisbane, Australia, pp. 199–206.

Ayala, J., Fourie, A., Reid, D., 2020a. Cone penetration testing on silty tailings using a new small calibration chamber. Géotechnique Lett. 10, 492–497. https://doi.org/10.1680/jgele.20.00037

Ayala, J., Fourie, A., Reid, D., 2020b. Development of a new large calibration chamber for testing thickened tailings with the cone penetration test, in: Quelopana, H. (Ed.), . Presented at the Paste 2020: 23rd International Conference on Paste, Thickened and Filtered Tailings, Gecamin Publications, Santiago. https://doi.org/10.36487/ACG_repo/2052_51

Ayala, J., Fourie, A., Reid, D., Jefferies, M., 2024. Inferring the state parameter from partially drained cone penetration test data using the soil behaviour-type index to adjust drained/undrained correlations. Presented at the Paste 2024: 26th International Conference on Paste, Thickened and Filtered Tailings, Australian Centre for Geomechanics, Perth, pp. 335–348.

Ayala, J., Martinelli, M., Reid, D., Fourie, A., 2023d. Cone resistance and soil state of tailing sand deposits using the Material Point Method. 10th Eur. Conf. Numer. Methods Geotech. Eng. NUMGE2023. https://doi.org/10.53243/NUMGE2023-195

Been, K., Crooks, J.H.A., Becker, D.E., Jefferies, M.G., 1986. The cone penetration test in sands: part I, state parameter interpretation. Géotechnique 36, 239–249.

Been, K., Jefferies, M.G., 1985. A state parameter for sands. Géotechnique 35, 99–112.

Been, K., Jefferies, M.G., Crooks, J.H.A., Rothenburg, L., 1987. The cone penetration test in sands: part II, general inference of state. Géotechnique 37, 285–299.

CIMNE, 2021. Computational analyses of Dam I failure at the Corrego de Feijao mine in Brumadinho Final Report.

DeJong, J.T., Randolph, M., 2012. Influence of Partial Consolidation during Cone Penetration on Estimated Soil Behavior Type and Pore Pressure Dissipation Measurements. J. Geotech. Geoenvironmental Eng. 138, 777–788. https://doi.org/10.1061/(ASCE)GT.1943-5606.0000646

Dienstmann, G., Schnaid, F., Maghous, S., DeJong, J., 2018. Piezocone Penetration Rate Effects in Transient Gold Tailings. J. Geotech. Geoenvironmental Eng. 144, 04017116. https://doi.org/10.1061/(ASCE)GT.1943-5606.0001822

Finnie, I.M.S., Randolph, M.F., 1994. Punch-through and liquefaction induced failure of shallow foundations on calcareous sediments. Presented at the Proc. 7th Int. Conf. on Behavior of Offshore Structures (BOSS '94), Boston, MA, pp. 217–230.

Fourie, A., Reid, D., Ayala, J., Russell, A., Vo, T., Rahman, M., Vinod, J., 2021. Improvements in estimating strengths of loose tailings: results from the TAILLIQ research project, in: Williams, D. (Ed.), . Presented at the Mine Waste and Tailings 2021 conference, The Australasian Institute of Mining and Metallurgy, Brisbane, Australia, pp. 207–217.

Fourie, A.B., Blight, G.E., Papageorgiou, G., 2001. Static liquefaction as a possible explanation for the Merriespruit tailings dam failure. Can. Geotech. J. 38, 707–719. https://doi.org/10.1139/t00-112

Fourie, A.B., Papageorgiou, G., 2001. Defining an appropriate steady state line for Merriespruit gold tailings. Can. Geotech. J. 38, 695–706. https://doi.org/10.1139/t00-111

Ghafghazi, M., Shuttle, D., 2008. Interpretation of sand state from cone penetration resistance. Géotechnique 58, 623–634. https://doi.org/10.1680/geot.2008.58.8.623

Ghasemi, P., Calvello, M., Martinelli, M., Galavi, V., Cuomo, S., 2018. MPM simulation of CPT and model calibration by inverse analysis.

Ghionna, V.N., Jamiolkowski, J.H., 1991. A critical appraisal of calibration chamber testing of sands, in: Huang, A.-B., Borden, R.H., Peterson, R.W., Thmay, M.T. (Eds.), . Presented at the Proceedings of the First International Symposium on Calibration Chamber Testing, Elsevier, New York, pp. 13–39.

Holden, J.C., 1991. History of the first six CRB calibration chambers, in: Huang, A.B. (Ed.), . Presented at the Proceedings of the First International Symposium on Calibration Chamber Testing, New York, pp. 1–12.

Houlsby, G.T., Hitchman, R., 1988. Calibration chamber tests of a cone penetrometer in sand. Géotechnique 38, 39–44. https://doi.org/10.1680/geot.1988.38.1.39

Huang, A., 1991. Calibration Chamber Testing, in: Elsevier (Ed.), . Presented at the Proceedings of the First International Symposium on Calibration Chamber Testing/ISOCCTl, Elsevier, Potsdam, New York.

ICMM, 2020. Global Industry Standard on Tailings Management.

ICOLD, 2001. Tailings dams: risk of dangerous occurrences: lessons learnt from practical experiences. Presented at the Commission Internationale des Grand Barrages, Paris.

Jefferies, M.G., Been, K., 2015. Soil Liquefaction: A Critical State Approach, 2nd ed, Applied Geotechnics Series. CRC Press, Boca Raton, FL.

Jefferies, M.G., Shuttle, D.A., 2005. NorSand: Features, Calibration and Use, in: Soil Constitutive Models. pp. 204–236. https://doi.org/10.1061/40771(169)9

Ladd, R., 1978. Preparing Test Specimens Using Undercompaction. Geotech. Test. J. 1, 16–23.

LePoudre, D.C., 2015. Examples, statistics and failure modes of tailings dams and consequences of failure. Presented at the Proceedings of the 2015 Canadian Dam Association Conference, Mississauga, Ontario, Canada.

Martinelli, M., Galavi, V., 2022. An explicit coupled MPM formulation to simulate penetration problems in soils using quadrilateral elements. Comput. Geotech. 145, 104697. https://doi.org/10.1016/j.compgeo.2022.104697

Martinelli, M., Galavi, V., 2020. Investigation of the Material Point Method in the simulation of Cone Penetration Tests in dry sand. Comput. Geotech. 103923.

Martinelli, M., Pisanò, F., 2022. Relating cone penetration resistance to sand state using the material point method. Géotechnique Lett. 12, 131–138. https://doi.org/10.1680/jgele.21.00145

Morgenstern, N.R., 2018. The Sixth Victor de Mello Lecture: Geotechnical risk, regulation, and public policy, in: Rochas, S.P. de G. e o C.B. de M. das (Ed.), . Presented at the Cobramseg 2018, Salvador, Bahia, Brazil, pp. 1–47.

Morgenstern, N.R., Vick, S.G., Van Zyl, D.V., 2015. Report on Mount Polley tailings storage facility breah. Report of independent expernet engineering investigation and review panel. Prepared on behalf of the Government of British Columbia and the Williams Lake and Soda Creek Indian Bands.

Plewes, H.D., Davies, M.P., Jefferies, M.G., 1992. CPT based screening procedure for evaluation liquefaction susceptibility. Presented at the 45th Canadian Geotechnical Conference, Canadian Geotechnical Society, Toronto, ON, pp. 41–49.

Riveros, G., Sadrekarimi, A., 2017. Static liquefaction analysis of the Fundao Dam failure. Presented at the GeoOttawa 2017, 70th Canadian Geotechnical Conference, Canadian Geotechnical Society, Ottawa, Canada.

Robertson, P., Campanella, R., 1983. Interpretation of cone penetration tests. Part II: Clay. Can. Geotech. J. 20, 734–745.

Robertson, P., Melo, L., Williams, D., Ward, G., 2019. Report of the Expert Panel on the Technical Causes of the Failure of Feijão Dam I.

Robertson, P.K., 2010. Estimating in-situ state parameter and friction angle in sandy soils from the CPT. Presented at the 2nd International Symposium on Cone Penetration Testing, Huntington Beach, CA.

Robertson, P.K., Campanella, R.G., 1983. Interpretation of cone penetration tests. Part I: Sand. Can. Geotech. J. 20, 718–733. https://doi.org/10.1139/t83-078

Robertson, P.K., Wride, C.E., List, B.R., Atukorala, U., Biggar, K.W., Byrne, P.M., Campanella, R.G., Cathro, D.C., Chan, D.H., Czajewski, K., Finn, W.D.L., Gu, W.H., Hammamji, Y., Hofmann, B.A., Howie, J.A., Hughes, J., Imrie, A.S., Konrad, J.M., Küpper, A., Law, T., Lord, E.R., Monahan, P.A., Morgenstern, N.R., Phillips, R., Piché, R., Plewes, H.D., Scott, D., Sego, D.C., Sobkowicz, J.C., Stewart, R.A., Watts, B.D., Woeller, D.J., Youd, T.L., Zavodni, Z., 2000. The CANLEX project: summary and conclusions. Can. Geotech. J. 37, 563–591. https://doi.org/10.1139/t00-046

Russell, A.R., Vo, T., Ayala, J., Wang, Y., Reid, D., Fourie, A.B., 2024. Cone penetration tests in saturated and unsaturated silty tailings. Géotechnique 74, 281–295. https://doi.org/10.1680/jgeot.21.00261

Shuttle, D., 2019. CPTwidget: a finite element program for soil-specific calibration of the CPT.

Shuttle, D., Jefferies, M., 2023. Discussion of "Improved cone penetration test predictions of the state parameter of loose mine tailings." Can. Geotech. J. 60, 1079–1081. https://doi.org/10.1139/cgj-2023-0003

Shuttle, D., Jefferies, M., 2016. Determining silt state from CPTu. Geotech. Res. 3, 90–118. https://doi.org/10.1680/jgere.16.00008

Shuttle, D., Jefferies, M., 1998. Dimensionless and unbiased CPT interpretation in sand. Int. J. Numer. Anal. Methods Geomech. 22, 351–391. https://doi.org/10.1002/(SICI)1096-9853(199805)22:5<351::AID-NAG921>3.0.CO;2-8

Shuttle, D.A., Cunning, J., 2007. Liquefaction potential of silts from CPTu. Can. Geotech. J. 44, 1–19. https://doi.org/10.1139/t06-086

Silva, M.F., Bolton, M.D., 2005. Interpretation of centrifuge piezocone tests in dilatant, low plasticity silts. Presented at the International Conference on Problematic Soils (GEOPROB 2005), Eastern Mediterranean Universoty, Famagusta, Cyprus, pp. 1–8.

Verdugo, R., Ishihara, K., 1996. The steady state of sandy soils. Soils Found. 36, 81–91.

Vick, S.G., 1990. Planning, design, and analysis of tailings dams. BiTech, Vancouver.

Wood, D.M., 1991. Soil Behaviour and Critical State Soil Mechanics. Cambridge University Press, Cambridge. https://doi.org/10.1017/CBO9781139878272

Yi, J.T., Goh, S.H., Lee, F.H., Randolph, M.F., 2012. A numerical study of cone penetration in fine-grained soils allowing for consolidation effects. Géotechnique 62, 707–719. https://doi.org/10.1680/geot.8.P.155